Thrombin-Induced Growth Cone Collapse: Involvement of Phospholipase A$_2$ and Eicosanoid Generation

Becky A. de la Houssaye, Keith Mikule, Dejan Nikolic, and Karl H. Pfenninger

Department of Cellular and Structural Biology, University of Colorado School of Medicine and University of Colorado Cancer Center, Denver, Colorado 80262

The studies presented here explore intracellular signals resulting from the action of repellents on growth cones. Growth cone challenge with thrombin or thrombin receptor-activating peptide (TRAP) triggers collapse via a receptor-mediated process. The results indicate that this involves activation of cytosolic phospholipase A$_2$ (PLA$_2$) and eicosanoid synthesis. The collapse response to repellents targets at least two functional units of the growth cone, the actin cytoskeleton and substratum adhesion sites. We show in a cell-free assay that thrombin and TRAP cause the detachment of isolated growth cones from laminin. Biochemical analyses of isolated growth cones reveal that thrombin and TRAP stimulate cytosolic PLA$_2$ but not phospholipase C. In addition, thrombin stimulates synthesis of 12- and 15-hydroxyeicosatetraenoic acid (HETE) from the released arachidonic acid via a lipoxygenase (LO) pathway. A selective LO inhibitor blocks 12/15-HETE synthesis in growth cones and inhibits thrombin-induced growth cone collapse. Exogenously applied 12(S)-HETE mimics the thrombin effect and induces growth cone collapse in culture. These observations indicate that thrombin-induced growth cone collapse occurs by a mechanism that involves the activation of cytosolic PLA$_2$ and the generation of 12/15-HETE.

Key words: growth cone; collapse; thrombin; signaling; phospholipase A$_2$; lipoxygenase

Chemorepellents provide important guidance cues for growth cones during nervous system development (Tessier-Lavigne and Goodman, 1996). Thrombin, a serine protease, was the first neurite repellent identified (Monard et al., 1983; Gurwitz and Cunningham, 1988; Hawkins and Seeds, 1986, 1989). However, it initially was thought to affect growth cones strictly by digestion of extracellular ligand or matrix molecules via its protease activity (Monard, 1988). Recent observations (Jalink and Moolenaar, 1992; Suidan et al., 1992) establish that the effects of thrombin on neurites are receptor-mediated. Thrombin activates its receptors by proteolytically unmasking the "tethered ligand," a peptide sequence near the N terminus of the receptor (Vu et al., 1991; Grand et al., 1996). Nonproteolytic thrombin receptor-activating peptides (TRAPs) representing the tethered ligand also can activate the receptor (Feng et al., 1995). At least two distinct thrombin receptors have been identified (Ishihara et al., 1997). That thrombin must play an important role in brain development and function is indicated by the finding that the genes encoding prothrombin, a thrombin receptor, and a thrombin antagonist (glial-derived nexin) are expressed in various brain regions, es-

pecially during development and in those regions known to exhibit plasticity (Mansuy et al., 1993; Niclou et al., 1994; Weinstein et al., 1995).

Maximum repellent stimulation causes growth cone "collapse," the withdrawal of lamellipodia and filopodia to form a club-shaped terminal structure (Kapfhammer and Raper, 1987). How repellent receptor activation causes this morphological change is unclear. Heterotrimeric G-proteins have been implicated in repellent signaling (Schwab, 1990; Igarashi et al., 1993; Grand et al., 1996; Moolenaar et al., 1997; Schindelholz and Reber, 1997), and so have receptor and other tyrosine kinases (Schindelholz and Reber, 1997; Smalheiser and Ali, 1994; Drescher et al., 1995; Brennan et al., 1997). Small Rho-family G-proteins are critical for reshaping the actin cytoskeleton in various cells and growth cones (Jalink et al., 1994; Gebbink et al., 1997; Jin and Strittmatter, 1997; Lamoureux et al., 1997; Tapon and Hall, 1997; Zipkin et al., 1997; Gallo and Letourneau, 1998; Katoh et al., 1998). Yet, we do not know whether growth cone collapse is caused primarily by cytoskeletal retraction (Stossel, 1993) followed by passive filopodial detachment, or whether dissociation of adhesion sites is a separate process triggered by the repellents. Because any form of amoeboid locomotion necessitates the coordinated attachment and detachment of pseudopods (Stossel, 1993; Huttenlocher et al., 1995), the involvement of an active detachment mechanism must be considered.

Nerve growth cones are enriched in high molecular weight, cytosolic phospholipase A$_2$ (cPLA$_2$; Nègre-Aminou et al., 1996), which may be involved in signaling (Dennis, 1994). Interestingly, PLA$_2$ and pseudopod activity may be correlated (Bar-Sagi and Feramisco, 1986; Bar-Sagi, 1989; Teslenko et al., 1997). In platelets, thrombin activates cPLA$_2$ and causes spreading (Grand et al., 1996). Does thrombin also stimulate growth cone cPLA$_2$, and is the cPLA$_2$ product arachidonic acid (AA) or one of its

eicosanoid derivatives involved in altering growth cone configuration?

Eicosanoids are synthesized through three different pathways involving cyclooxygenases (generating prostaglandins), cytochrome P-450 monooxygenases, or lipoxygenases [LOs; synthesizing hydroperoxyeicosatetraenoic acids (HPETEs) and leukotrienes; Smith, 1989; Capdevila et al., 1992; Yamamoto et al., 1997]. HPETEs are reduced to hydroxyeicosatetraenoic acids (HETEs). 12(*S*)-HETE is of particular interest, because several reports link its function to pseudopod activity or cell motility (Goetzl et al., 1977; Yoshino et al., 1993; Ferrante et al., 1994). In endothelial and certain cancer cells 12(*S*)-HETE induces disruption of adhesion sites and process retraction (Tang et al., 1993; de la Houssaye et al., 1997).

The present studies test the hypotheses that (1) cPLA$_2$ activation and 12-HETE generation are necessary for thrombin-induced growth cone collapse; (2) 12-HETE mimics the thrombin response; and (3) a signaling pathway involving cPLA$_2$ and 12/15-LO regulates growth cone detachment (de la Houssaye et al., 1997; Mikule et al., 1997).

MATERIALS AND METHODS

Materials. Free AA was purchased from Sigma (St. Louis, MO), and L-stearoyl-2-arachidonyl-*sn*-glycerol (DG) was from Avanti Polar Lipids (Alabaster, AL). L-α-Stearoyl-2-[^{14}C]arachidonyl-phosphatidylinositol ([^{14}C]AA-PI; 20–40 mCi/mmol), -phosphatidylethanolamine ([^{14}C]AA-PE; 40–60 mCi/mmol), and -phosphatidylcholine ([^{14}C]AA-PC; 40–60 mCi/mmol) were obtained from DuPont New England Nuclear (Boston, MA) as was [^{3}H]AA. Reagents for chemiluminescence were from the same vendor. Analytical grade solvents for routine thin-layer-chromatography (TLC) analysis and tissue culture dishes were purchased from Fisher Scientific (Pittsburgh, PA). 2,3-Butanedione monoxime (BDM), *N*-Tris-[hydroxymethyl]-methyl-2-aminoethanesulfonic acid (TES), thrombin, and other chemicals were from Sigma. Aprotinin was from Calbiochem (San Diego, CA). Polyacrylamide, prestained molecular weight standards, and other reagents for SDS-PAGE were from Life Technologies (Grand Island, NY). Tissue culture media and laminin were also from Life Technologies. 12(*S*)- and 15(*S*)-HETE, nordihydroguaiaretic acid (NDGA), cinnamyl-3,4-dihydroxy-α-cyanocinnamate (CDC), and indomethacin were purchased from Biomol (Plymouth Meeting, PA). TRAP came from Peninsula Laboratories (San Carlos, CA). TLC plates were obtained from EM Science (Gibbstown, NJ) and Whatman (Clifton, NJ). Sprague Dawley rats were from Harlan (Indianapolis, IN). Solid phase extraction columns were purchased from J. T. Baker (Phillipsburg, NJ). Rabbit antibodies to platelet 12-LO and to leukocyte 12/15-LO were from Oxford Biomedical Research (Oxford, MI) and Cayman Chemical (Ann Arbor, MI), respectively. HRP-conjugated goat anti-rabbit antibody was purchased from Vector Laboratories (Burlingame, CA). Texas Red-conjugated phalloidin and Slow-Fade Light were products of Molecular Probes (Eugene, OR). Insulin and insulin-like growth factor 1 (IGF-1) were from Collaborative Biomedical Products (Bedford, MA), and brain-derived neurotrophic factor (BDNF) was from Amgen (Thousand Oaks, CA).

Neuron culture. Cerebral cortices were dissected from embryonic day 18 Sprague Dawley rats, cut into explants of <1mm^3, and cultured on either poly-D-lysine-coated coverglass (Assistent) or poly-D-lysine-coated tissue culture plastic. After 24 hr in B27 neurobasal medium (NB) supplemented with 10% fetal bovine serum, cultures were switched to serum-free B27 NB. The cultures were incubated at 37°C in 5% CO$_2$ in air. Sprouting neurons were observed readily on day 1. On day 2 or 3, long neurites were present, and the cultures were used for collapse experiments.

Actin staining. After experimentation, cultures were fixed by slow infusion of fixative (4% paraformaldehyde in 0.1 M phosphate buffer, pH 7.4) into the culture dishes over 10 min (Pfenninger and Maylié-Pfenninger, 1981). Thereafter, the fixative was removed by rinsing three times with PBS containing 1 mM glycine. Cultures were then blocked with PBS and 1% bovine serum albumin (BSA) and permeabilized by incubation in 0.02% Triton X-100 for 5 min. After three washes in PBS and BSA, cultures were incubated with Texas Red-conjugated phalloidin for 30 min. Unbound phalloidin was washed away by two PBS rinses,

after which the coverglasses were mounted in Slow-Fade Light on microscope slides. Images were recorded on 35 mm film using a Zeiss (Thornwood, NY) Axiophot fluorescence microscope equipped with epiillumination.

Growth cone collapse assay. Before repellent factor treatment, some of the day 2–3 explant cultures were preincubated (at 37°C) with inhibitor or vehicle control (dimethylsulfoxide or ethanol) for 30–60 min. Cultures were then challenged with a repellent factor or vehicle control for 1–30 min. In some experiments, live cultures were photographed with a Zeiss IM 35 inverted photo microscope equipped with a stage heater, whereas in others cultures were fixed (as above) after 7 min of repellent factor treatment. Growth cone collapse was assessed quantitatively in aldehyde-fixed cultures by grading the degree of collapse in a large number of randomly selected growth cones. Because growth cones of control neurons exhibited a heterogenous phenotype and some of the collapse responses (at 7 min) were graded, binary assignments (collapsed or intact) were inadequate for these analyses. Therefore, we classified growth cones into one of four categories: fully spread, "veiled" growth cones (1, "spread and veiled"), spread-out growth cones with prominent filopodia but reduced veiling (2, "reduced veiling"), growth cones without lamellipodia and possessing only few filopodia (3, "partially collapsed"), and fully collapsed, club-shaped neurite termini (4, "club-shaped"). The numbers assigned to the classes were used to determine a "collapse index" for each experimental condition by calculating a weighted average for each growth cone population analyzed. The resulting collapse indices were averaged for the same condition, and SEMs were determined. Student's *t* test was used to assess statistical significance of values for different conditions.

Growth cone particle isolation. Growth cone particles (GCPs) were prepared as described by Pfenninger et al. (1983) and modified by Lohse et al. (1996). Briefly, 18 day fetal brains were homogenized in ∼8 volumes of 0.32 M sucrose containing 1 mM MgCl$_2$, 2 mM TES buffer, pH 7.3, and 3 μM aprotinin. A low-speed supernatant (1660 × *g* for 15 min) was loaded onto a discontinuous sucrose density gradient with steps of 0.83 and 2.66 M sucrose containing MgCl$_2$ and TES. The gradients were spun to equilibrium at 242,000 × *g* for 40 min in a vertical rotor (Vti50; Beckman Instruments, Palo Alto, CA). The GCP fraction at the 0.32–0.83 M sucrose interface was collected and used for the experiments described below.

GCP release assay. Petri dishes (35 mm diameter) were coated with 10 μg of mouse laminin in PBS by incubation at room temperature for 60 min with shaking. Dishes were subsequently rinsed three times with PBS to remove unbound laminin and then blocked with 5% nonfat dry milk (Carnation) in PBS for 30 min. After three PBS rinses to remove the blocking agent, the dishes were ready for the addition of GCPs. Before plating, the GCP fraction was slowly added at 4°C to an equivalent volume of 2× concentrated, modified Krebs' buffer (22 mM sucrose, 50 mM NaCl, 5 mM KCl, 22 mM HEPES, pH 7.4, 10 mM glucose, 1.2 mM NaH$_2$PO$_4$, 1.2 mM MgCl$_2$, and 2 mM CaCl$_2$). After incubation for 5 min at 37°C, this buffered GCP preparation was added to the laminin-coated Petri dishes. Contact with the substratum was facilitated by centrifuging the dishes for 15 min at 5000 × *g* (Beckman JS5.2 rotor) at room temperature, followed by incubation at 37°C to allow adhesion site formation. After 10 min, unattached GCPs were removed by rinsing the dishes twice with 1× modified Krebs' buffer. Plated GCPs were then challenged with repellent factor (TRAP or thrombin) for 20 min at 37°C. The supernatant containing released GCPs was collected and centrifuged for protein determination of the pellet. GCPs that remained attached after repellent treatment were removed with 5% SDS for protein assay. Protein was measured according to the method of Lowry et al. (1951) as modified by Peterson (1983). Results of these experiments were expressed as the percentage of released versus total GCP protein initially attached minus release in untreated samples.

Gel electrophoresis and Western blotting. SDS-PAGE was performed according to the method of Laemmli (1970) using 5–15% acrylamide gradients. The GCP fraction was diluted threefold to fourfold with 0.32 M sucrose buffer and spun for 30 min at 39,800 × *g*. Protein amounts in the pellets were determined by dye-binding assay (Bradford, 1976). Polypeptides of pelleted GCPs (30 μg/lane) were resolved by SDS-PAGE. Prestained standards were used to determine apparent molecular mass. Resolved proteins were transferred to nitrocellulose essentially as described by Towbin et al. (1979), with a semidry blotting apparatus for 60 min at 300 mA for a 14 × 17 cm gel. Ponceau S staining served to monitor the efficiency of protein transfer. Blots were then rinsed in PBS
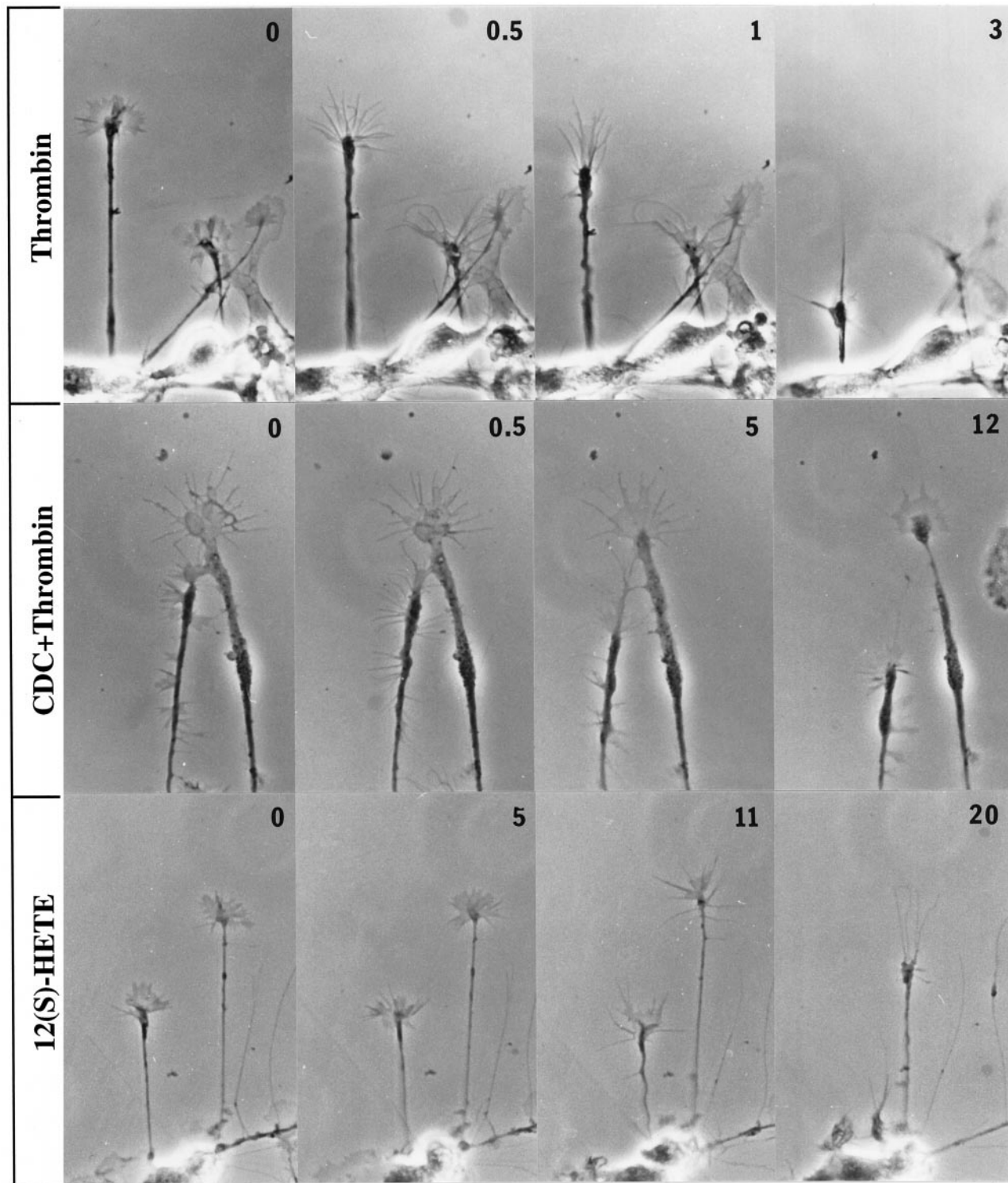
Figure 1. Effects of thrombin, thrombin plus LO inhibitor, and 12(*S*)-HETE on growth cone configuration. Phase-contrast micrographs are shown of cultures of embryonic day 18 rat cortical neurons that were either pretreated with vehicle alone or inhibitor for 45 min before challenge with thrombin or 12(*S*)-HETE. *Numbers* in the *top right corners* indicate time in minutes of exposure to collapsing reagent. *Top* to *bottom*, 100 nM thrombin, 10 μM CDC pretreatment (30 min) followed by 100 nM thrombin, and 10^{-7} M 12(*S*)-HETE. The large growth cone in *CDC+Thrombin* exhibits at 0 min (which is a CDC-alone control) and at 0.5 min vertically extended veils. By 5 min they have disappeared.

and distilled water and dried. Before incubation with primary antibody, blots were blocked with 5% nonfat milk powder and 0.02% Tween 20 in PBS for 2 hr at room temperature. Blots were probed in the same blocking solution and conditions with either polyclonal rabbit anti-platelet or polyclonal rabbit anti-leukocyte 12-LO antibody at 1:2000 or

1:5000, respectively. Blots were washed five times in blocking solution, followed by incubation with secondary antibody (HRP-conjugated goat anti-rabbit antibody at 1:5000) for 1 hr in blocking solution. After extensive washing, bound antibody was detected by enhanced chemiluminescence according to the manufacturer's directions (New England
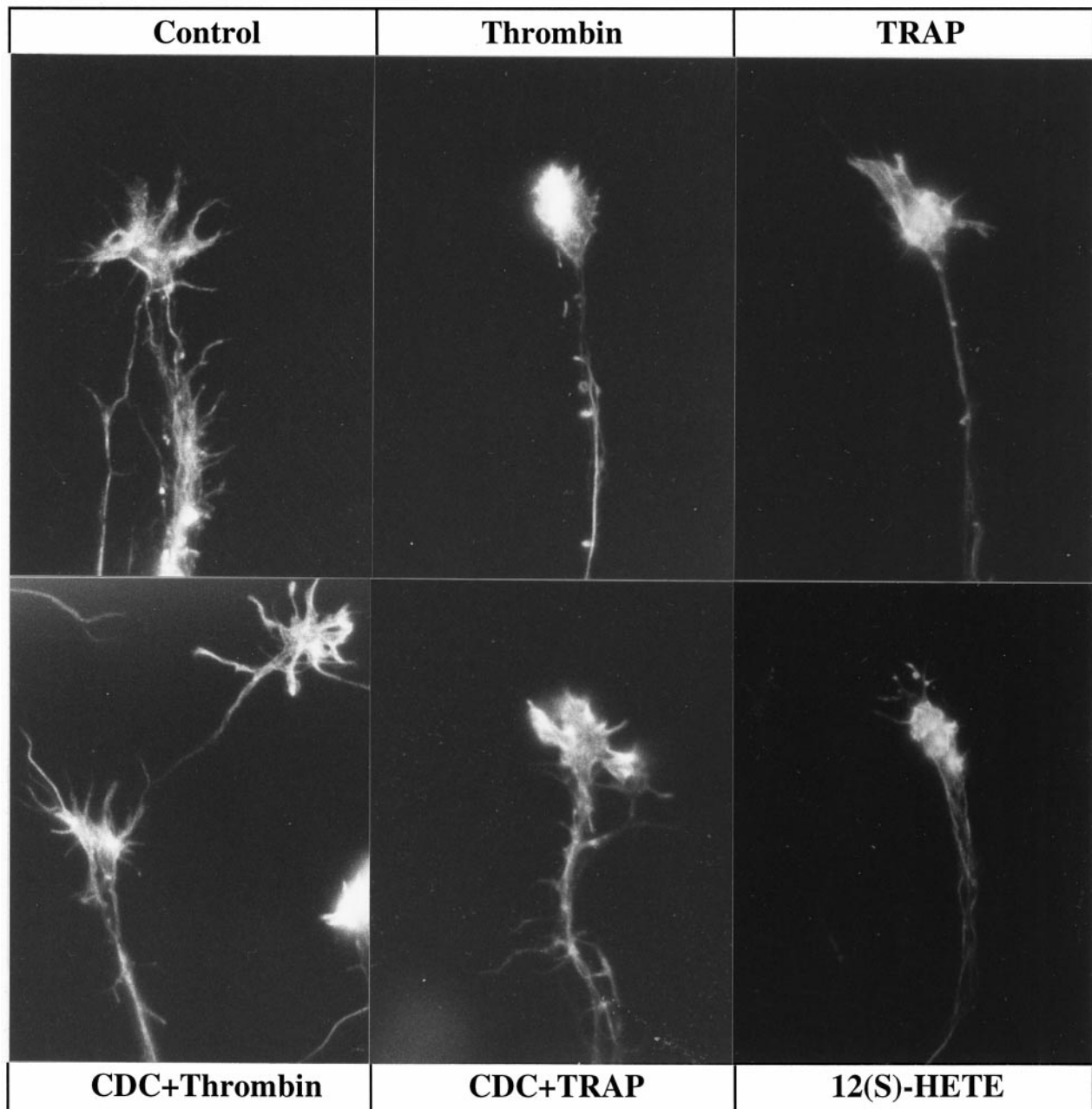
Figure 2. Effects of thrombin, TRAP, thrombin or TRAP plus LO inhibitor, and 12(*S*)-HETE on filamentous actin in growth cones. Cultured El8 rat cortical neurons were fixed and stained with Texas Red-conjugated phalloidin after the following experimental treatments: control (vehicle alone), thrombin (100 nM) for 7 min, TRAP (100 μM) for 7 min, 45 min pretreatment with CDC (10 μM) followed by thrombin (100 nM) or TRAP (100 μM) for 7 min, and 12(*S*)-HETE (10^{-7} M) for 12 min. Thrombin and TRAP cause collapse, but the TRAP effect, although clear-cut, is not as dramatic as that of thrombin; CDC inhibits or significantly attenuates collapse, and 12(*S*)-HETE mimics the effects of thrombin and TRAP.

Nuclear) by contact-exposing x-ray film (X-OMAT Blue XB-1; Eastman Kodak, Rochester, NY).

Phospholipase assays. For PLA_2 assays, GCPs suspended in modified Ca^{2+}-free Krebs' buffer (10–30 μg protein/assay) were first incubated for 10 min on ice in the presence or absence of effectors. Subsequently, phospholipid substrate (PC, PE, or PI) containing radiolabeled AA (7–14 μM; 50,000–100,000 cpm/assay) was added, and the reaction was performed at 37°C for 10 min. Typically, assay mixtures contained 10 μM $CaCl_2$; specific modifications are described in the figure legends. For phospholipase C (PLC) assays, conditions were the same when run in parallel with PLA_2 assays. When PLC assays were run independently, Ca^{2+} was increased to 1 mM. Reactions were terminated by the addition of 3.75 volumes of cold chloroform/methanol (1:2). PLA_2 assays also

were performed on neurons dissociated from fetal rat cerebral cortex. The assay conditions were the same as those just described for GCPs.

Extraction of phospholipase products was performed according to the method of Bligh and Dyer (1959). Products recovered in chloroform were loaded onto Silica Gel 60 TLC plates and developed as described earlier (Nègre-Aminou and Pfenninger, 1993) in hexane/ether/acetic acid (40:60:1). AA and DG were identified on TLC by co-migration with authentic standards. The appropriate bands were excised into scintillation fluid and counted on a Beckman LS 1801 scintillation spectrometer. All assays were run in triplicate.

Eicosanoid assays. Eicosanoid production in GCPs was measured by metabolic labeling from ^{3}H-AA or ^{14}C-AA-PC or by mass spectrometric detection. To determine HETE synthesis by radiolabeling, assays were

run essentially as for PLA$_2$ except that phospholipid substrate was increased to 100,000 cpm/assay, and assay time at 37°C was 15 min. To measure LO activity directly, without PLA$_2$ involvement, ^{3}H-AA was the substrate of choice. Reactions were stopped by the addition of chloroform/methanol as for the phospholipase assays. Reaction products were extracted as described by Birkle et al. (1988) and spotted on preactivated Silica Gel 60 TLC plates, and the plates were developed in the upper phase of ethyl acetate/isooctane/acetic acid/water (100:60:20:100). AA and HETEs were identified by co-migration with standards. Appropriate bands were counted by liquid scintillation spectrometry.

For identification of HETEs we used a liquid chromatography–tandem mass spectrometry (LC–MS–MS) strategy. The reaction substrate consisted of 3.5 μM AA, with the addition of 3.5 μM deuterated AA (D$_8$-AA) plus 1 μCi [^{3}H]AA to track reaction products by mass and radioactivity, respectively. Reactions were stopped with ice-cold ethanol; the mixtures were kept overnight at -20°C under N$_2$; and the proteins were spun out. The supernatants were diluted with H$_2$O and loaded onto 1 ml C$_{18}$ Sep-Pak columns (Varian, Palo Alto, CA). After washing with H$_2$O, eicosanoid was eluted with 2 ml of methanol. These samples were resolved by reverse-phase HPLC, and the eluted fractions were analyzed on-line by a tandem quadrupole mass spectrometer (API-III+; Perkin-Elmer Sciex, Thornhill, Ontario, Canada; MacMillan and Murphy, 1995). Collision-induced decomposition of HETE regioisomers produced characteristic fragment ions that were identified at the second MS stage.

RESULTS

Growth cone collapse in culture

Experiments were performed on growth cones in cultures of rat cerebral cortex to assess qualitatively and quantitatively the collapsing effects of thrombin and the nonproteolytic TRAP, with or without inhibitors of AA metabolism. Figure 1 shows the effect of thrombin treatment on growth cones at different times. Almost immediately thrombin causes disappearance of lamellipodia and, after several minutes, filopodia. After 5–10 min, most growth cones are fully collapsed, and neurite length is reduced. By 30 min neurite beading is observed (results not shown). TRAP was used at a concentration ~1000 times higher than that of thrombin, consistent with data on receptor binding and TRAP activation in other systems (Feng et al., 1995; also see Natarajan et al., 1995; Grand et al., 1996). TRAP has qualitatively the same effect as thrombin, but the change is not as pronounced, and neurite beading is not seen routinely. The collapse phenomenon is shown at higher magnification in Figure 2, after staining of filamentous actin with Texas Red-conjugated phalloidin. Control growth cones exhibit spread-out veils and/or filopodia with filamentous actin abundant in the periphery, whereas thrombin or TRAP treatment causes withdrawal of lamellipodia and filopodia and actin redistribution from the peripheral to the proximal growth cone.

To test for the putative role of PLA$_2$ in thrombin and TRAP signaling, one would ideally inhibit or activate growth cone PLA$_2$. However, the molecular identities of growth cone PLA$_2$s have not been established, and selective inhibitors that block these enzymes are not known. Therefore, we proceeded with experiments involving inhibitors of the metabolism of the PLA$_2$ product AA. Indomethacin is a specific blocker of cyclooxygenases, thereby inhibiting the synthesis of prostaglandins and related eicosanoids (Salari et al., 1984), and has no effect on control or thrombin treatment of growth cones (data not shown). CDC (Cho et al., 1991; Wen et al., 1996) is a selective inhibitor of LOs, including 12-LO, which catalyzes the synthesis of 12(S)- and some 15(S)-HETE. CDC alone does not alter growth cone structure qualitatively (Fig. 1, *CDC+Thrombin, 0* min) or quantitatively (the collapse index for CDC alone, 30 min, is 1.42 for 100 growth cones vs 1.34 for controls; see Table 1). However, pretreatment with CDC inhibits the thrombin effect on growth cones (Figs. 1,

Table 1. Comparison of growth cone collapse indices

Condition	Collapse index $\pm$ SEM[a]
Control	1.34 ± 0.05
Thrombin	3.22 ± 0.06*
CDC/thrombin	2.32 ± 0.16**
TRAP	2.83 ± 0.12*
12(S)-HETE	2.92 ± 0.12*

[a]Data are calculated from those shown in Figure 4. Values close to 1.0 indicate intact growth cones; those close to 4.0 indicate completely collapsed growth cones.

*Values significantly different from control ($p < 10^{-4}$ in Student's *t* test).

**Value significantly different from thrombin treatment alone ($p < 0.0075$ in Student's *t* test).
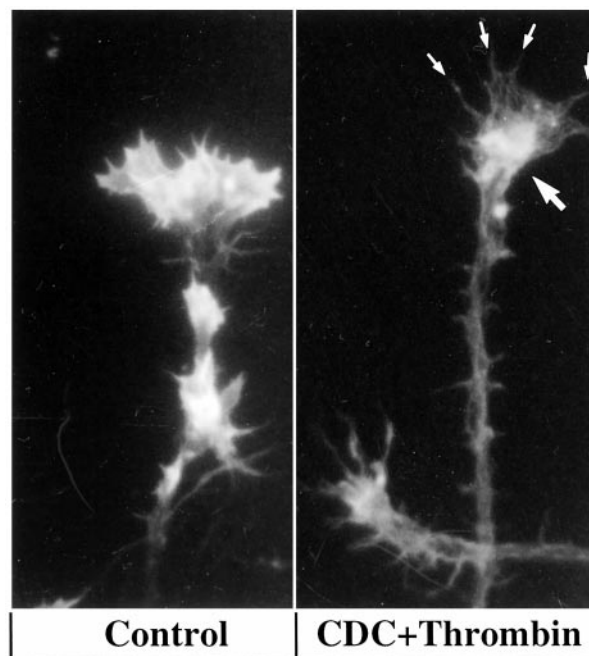

Figure 3. The LO inhibitor CDC inhibits thrombin-induced shape change of the growth cone but may allow redistribution of the actin cytoskeleton. *A*, Growth cones fixed and stained with Texas Red-conjugated phalloidin after control (vehicle alone) incubation. *B*, 30 min CDC (10 μM) pretreatment followed by thrombin challenge (100 nM) for 7 min. *Small arrows* indicate intact filopodia with diminished actin staining. The *large arrow* denotes "clumped" actin filaments in the proximal growth cone.

2). Although thrombin collapses growth cones even after incubation with indomethacin, CDC-pretreated growth cones retain their spread-out appearance. A more potent but less selective inhibitor of all LOs, NDGA (Salari et al., 1984), also protects growth cones from thrombin- or TRAP-induced collapse (data not shown).

Figures 2 and 3 allow for comparison of phalloidin-stained growth cones in control cultures and in cultures challenged with thrombin or TRAP after CDC incubation. Again, growth cones treated with CDC alone (data not shown) are not distinguishable from controls. CDC-pretreated growth cones challenged with thrombin typically retain their spread-out shape with actin-rich, attached filopodia and lamellipodia. In some cases, however, we observed fully spread growth cones with filamentous actin largely depleted from lamellipodia and filopodia and clumped in the proximal body (Fig. 3). Some actin depolymerization may have taken place as well.
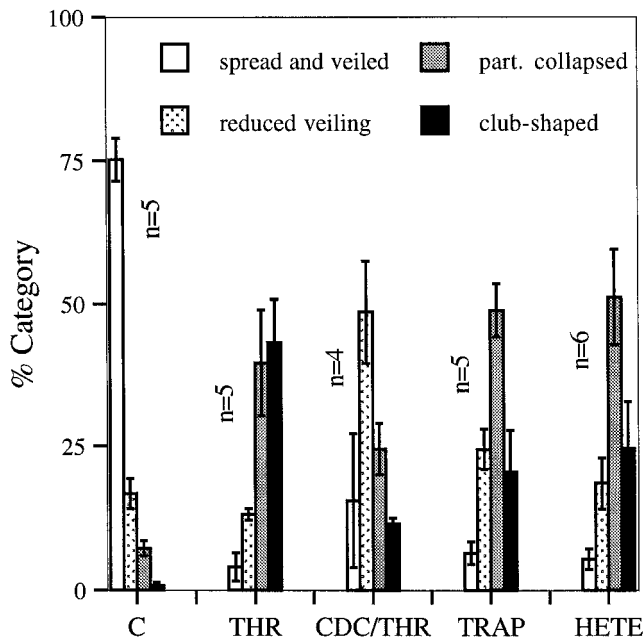
Figure 4. Quantitative analysis of growth cone collapse induced by thrombin (with or without CDC pretreatment), TRAP, or 12(*S*)-HETE. Collapse status was assessed on fixed neural cultures having undergone the following treatments: *C*, control, vehicle alone; *THR*, thrombin (100 nM) for 7 min; *CDC/THR*, CDC (10 μM) pretreatment for 30 min, followed by thrombin (100 nM) for 7 min; TRAP (100 μM) for 7 min; and 12(*S*)-HETE (10^{-7} M) for 10 min. For each condition at least 200 growth cones from at least four independent experiments were scored as described in Materials and Methods. Data are presented as percent of total growth cones observed. Error bars indicate SEM; *n*, number of independent experiments.

The results of these experiments have been analyzed quantitatively. At least 50 randomly selected growth cones in each of four to six independent experiments were classified into four different categories: spread and veiled, reduced veiling, partially collapsed, and club-shaped (see Materials and Methods). These categories are exemplified by the main growth cone in Figure 1 (thrombin treatment) at 0–3 min. Figure 4 shows a shift of growth cones from predominantly intact (controls) to predominantly collapsed (thrombin or TRAP) and the strong attenuation of this effect by CDC. Collapse indices for the different experimental conditions are shown in Table 1 and were used to determine that thrombin- and TRAP-induced collapse was highly significant, as was its attenuation by CDC.

If 12-LO is necessary for at least a part of the collapsing action of thrombin and TRAP, as the experiments with CDC suggest, then the primary 12-LO product 12(*S*)-HETE should mimic the effect of thrombin and TRAP. This is shown qualitatively in Figures 1 and 2 and quantitatively in Figure 4 and Table 1. In this system at 10^{-7} M, 12(*S*)-HETE does indeed cause growth cone collapse that is morphologically very similar to the effect of thrombin and TRAP. 12(*S*)-HETE-induced collapse is highly significant but less dramatic than that of thrombin (see Fig. 4, Table 1), and the neurite beading seen after 30 min of maximum thrombin exposure is observed only rarely. The collapse effect of 12(*S*)-HETE is not affected by growth cone pretreatment with the LO inhibitor CDC (data not shown).

Growth cone detachment

Collapsing factors must affect the cytoskeleton of the growth cone as well as filopodial and lamellipodial attachment to the
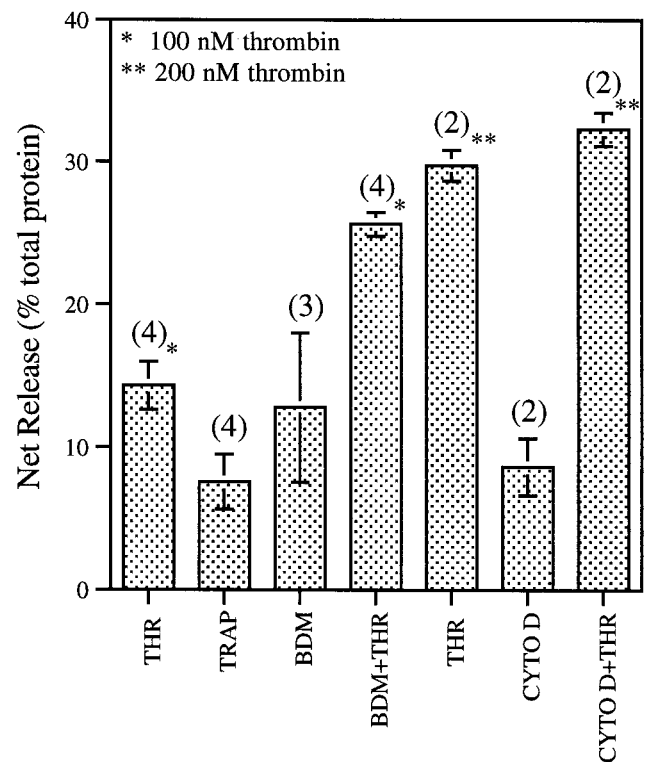

Figure 5. Thrombin- and TRAP-induced detachment of GCPs from a laminin substratum. GCPs plated on laminin were exposed for 20 min to thrombin (*THR*, 100 or 200 nM), to vehicle with or without cytochalasin D (*CYTO D*, 1 μM) or BDM (20 mM) pretreatment, or to TRAP (100 μM). Detachment was measured as pelletable protein collected in the supernatant. Data are net increases $\pm$ SEM above untreated controls, expressed as percent of total GCP protein bound initially. In control conditions detachment was 15.2 $\pm$ 6.9% (average $\pm$ SD) of total GCPs plated. *Numbers* in *parentheses* indicate numbers of independent experiments.

substratum. To analyze this latter phenomenon, we designed a cell-free substrate detachment assay involving so-called GCPs isolated from fetal rat brain (Pfenninger et al., 1983). GCPs contain a full complement of growth cone organelles, are viable for at least 1 hr after isolation (Lockerbie et al., 1991), and have been shown to be derived primarily from axonal growth cones (Lohse et al., 1996). When GCPs attached to laminin were exposed to thrombin, many of them detached from the substratum and could be collected in the supernatant (Fig. 5). Thrombin-induced detachment was detectable at $\geq$50 nM and reached a plateau between 200 and 300 nM (data not shown), indicating dose dependence. TRAP mimicked the thrombin effect, demonstrating that protease activity is not required for detachment.

GCPs contain a substantial actin meshwork (Pfenninger et al., 1983). Despite their small size ($\sim$0.3–0.5 μm diameter), contraction of the actin–myosin system could be responsible for at least some of the detachment effect observed in the assay. Therefore, laminin-attached GCPs were first treated for 20 min at 37°C with 1 μM cytochalasin D to depolymerize the actin cytoskeleton or with 20 mM BDM to inhibit selectively myosin ATPase (Cramer and Mitchison, 1995). Both reagents caused considerable release of GCPs by themselves (Fig. 5), consistent with known effects on cell spreading (Mooney et al., 1995; Sanders et al., 1999). However, thrombin challenge increased detachment further ($p <$ 0.018 for BDM; $p <$ 0.0047 for cytochalasin D). The release by

Table 2. PLA$_2$ activity in neurons and growth cones: whole neurons versus GCPs

Condition	Concentration (nM)	Substrate	Net activity (pmol · min^{-1} · mg protein^{-1})	
			Intact neurons	GCPs
Control		PI	0.6 ± 0.45	37.9 ± 1.1
		PE	4.4 ± 0.99	25.7 ± 2.3
Thrombin	200	PI	42.5 ± 16	262 ± 47
		PE	26.8 ± 1.9	210.2 ± 4.8

Data are from representative experiment done in triplicate (values are means ± SD). All measurements were obtained in the same experiment and share the control indicated.

the combined treatments equals the sum (for BDM) or is within the error range of the sum (for cytochalasin D) of the separate treatments.

Phospholipase activation

Our hypothesis predicts that one of the important steps in thrombin-induced growth cone collapse is the activation of cytosolic PLA$_2$. Therefore, we studied PLA$_2$ activation in primary neurons and in GCPs isolated from fetal rat brain. Because these assays have to be performed on cellular systems with endogenous phospholipid present, one cannot readily measure absolute enzyme activities. However, comparisons of the hydrolysis of exogenous, radiolabeled substrates enable one to determine relative PLA$_2$ activities in comparable experiments. In PLA$_2$ assays performed on primary neurons dissociated from cerebral cortex, thrombin greatly stimulated AA release from PE or PI, as shown in Table 2. Because of the specific effect of thrombin on growth cones and because of the enrichment of PI-selective PLA$_2$ in growth cones (Nègre-Aminou et al., 1996), we proceeded with the more detailed analysis of PLA$_2$ activation in GCPs. Data are shown primarily for PI as a substrate, because PI is the phospholipid with the highest level of AA turnover in growth cones (Nègre-Aminou and Pfenninger, 1993). Table 2 shows that, under comparable experimental conditions, thrombin stimulates PLA$_2$ in GCPs to much higher levels of free AA than in whole neurons. Figure 6 shows the release of AA from PI as a function of increasing concentrations of thrombin or TRAP. We observed a high level of activation (from fivefold to sevenfold) saturating at ~250 nM for thrombin. TRAP also clearly stimulated PLA$_2$, but to a considerably lesser degree and at a ~1000-fold higher concentration.

We had determined previously that GCPs contain very little, if any, secreted PLA$_2$ (Nègre-Aminou et al., 1996). To exclude the possibility that thrombin stimulated the release of a secreted PLA$_2$ we performed PLA$_2$ assays in the presence of reducing agent, which inactivates the catalytic domain of all secreted forms of the enzyme. As Table 3 shows, dithiothreitol (DTT) does not reduce the control or thrombin-stimulated levels of PLA$_2$ activity. Data are shown for PI, but the same observations were made for PE and PC (data not shown). This confirms the role of high molecular weight PLA$_2$ in the cytosol in a thrombin-activated pathway.

The PLA$_2$ response to thrombin is calcium-dependent in permeabilized GCPs, as shown in Figure 7. In the presence of EGTA, there is no stimulation of enzyme activity, whereas the

thrombin response reaches a maximum at ~100 μM Ca^{2+}, without much change in basal, nonstimulated conditions.

In a previous publication (Nègre-Aminou et al., 1996), we reported that GCPs contain at least two biochemically separable PLA$_2$ activities selective for PI and PE, respectively. Under experimental conditions used at the time, PC hydrolysis in GCPs was at background level without stimulation. However, Figure 8 shows that thrombin stimulates AA release from all three phospholipid substrates but at different levels, ranging from approximately fivefold for PI to approximately sevenfold for PC. These values do not take into account, however, known differences in the abundance of endogenous phospholipid substrates and/or potential competition among the PLA$_2$s for a given substrate.

In other systems, such as platelets, thrombin has been reported to activate PLC (Crouch and Lapetina, 1988; Huang et al., 1991). Therefore, we measured DG release from PI in parallel to AA release. Figure 9 shows that thrombin inhibits DG release, rather than stimulating it, and that the effect is calcium-dependent in a manner similar to the stimulation of PLA$_2$. To ascertain the authenticity of thrombin-induced PLC inhibition, we compared the effects of thrombin and IGF-1 on PLA$_2$ and PLC in GCPs. GCPs are known to be rich in IGF-1 receptors (Quiroga et al., 1995), and IGF-1 is known to activate PLC in many systems (Poiraudeau et al., 1997). Figure 10 shows AA and DG release from PI (at 10 μM free Ca^{2+}) in response to different concentrations of IGF-1. In the low nanomolar range, IGF-1 does indeed stimulate DG release in GCPs approximately twofold (Fig. 10). IGF-1 also stimulates AA release from PI, but only ~1.7-fold. This activation of PLA$_2$ is a much weaker response than that observed with thrombin (see Figs. 6, 8).

Because of the mild stimulation of PLA$_2$ by IGF-1, we assayed for PLA$_2$ activation by other trophic factors whose receptors are known to be present on growth cones or to be linked to PLA$_2$ stimulation in other cellular systems. (In these experiments, shown in Tables 2–4, net control levels of PLA$_2$ activity in GCPs range from 38 to 107 pmol AA released · min^{-1} · mg of protein^{-1}, probably because of slight variations in the GCP fraction. However, data sets are shown always with controls measured in the same experimental series.) TrkB, the receptor for BDNF, is readily detectable by immunoblot and enriched in GCPs isolated from whole fetal brain (K. H. Pfenninger and S. Ross, unpublished results). However, BDNF did not significantly stimulate PLA$_2$ activity in GCPs (Table 4). BDNF combined with IGF-1 or insulin alone also failed to stimulate PLA$_2$ significantly in our assays (Table 4). When these experiments were performed with PE or PC as substrates, AA release again was only marginally or not at all increased (data not shown).

Generation of eicosanoids

The effect of CDC in collapse and growth cone detachment assays suggests that eicosanoid synthesis from AA is an important step in thrombin and TRAP signaling. Lipid extracts prepared in acid conditions can be resolved by TLC to separate 12/15-HETE (which co-migrate) from the other compounds, including AA, DG, and 5-HETE (Birkle et al., 1988). With this approach we studied the generation of HETE in GCPs, without or with thrombin stimulation. Figure 11*A* shows, in assays involving [^{14}C]AA-PC as a substrate, the generation of AA and of a compound co-migrating in TLC with 12- or 15-HETE. As seen already, there is substantial stimulation of AA release by thrombin. Radioactivity co-migrating with 12-HETE also is increased, ~2.5-fold above control (Fig. 11*B*). The selective 12-LO inhibitor
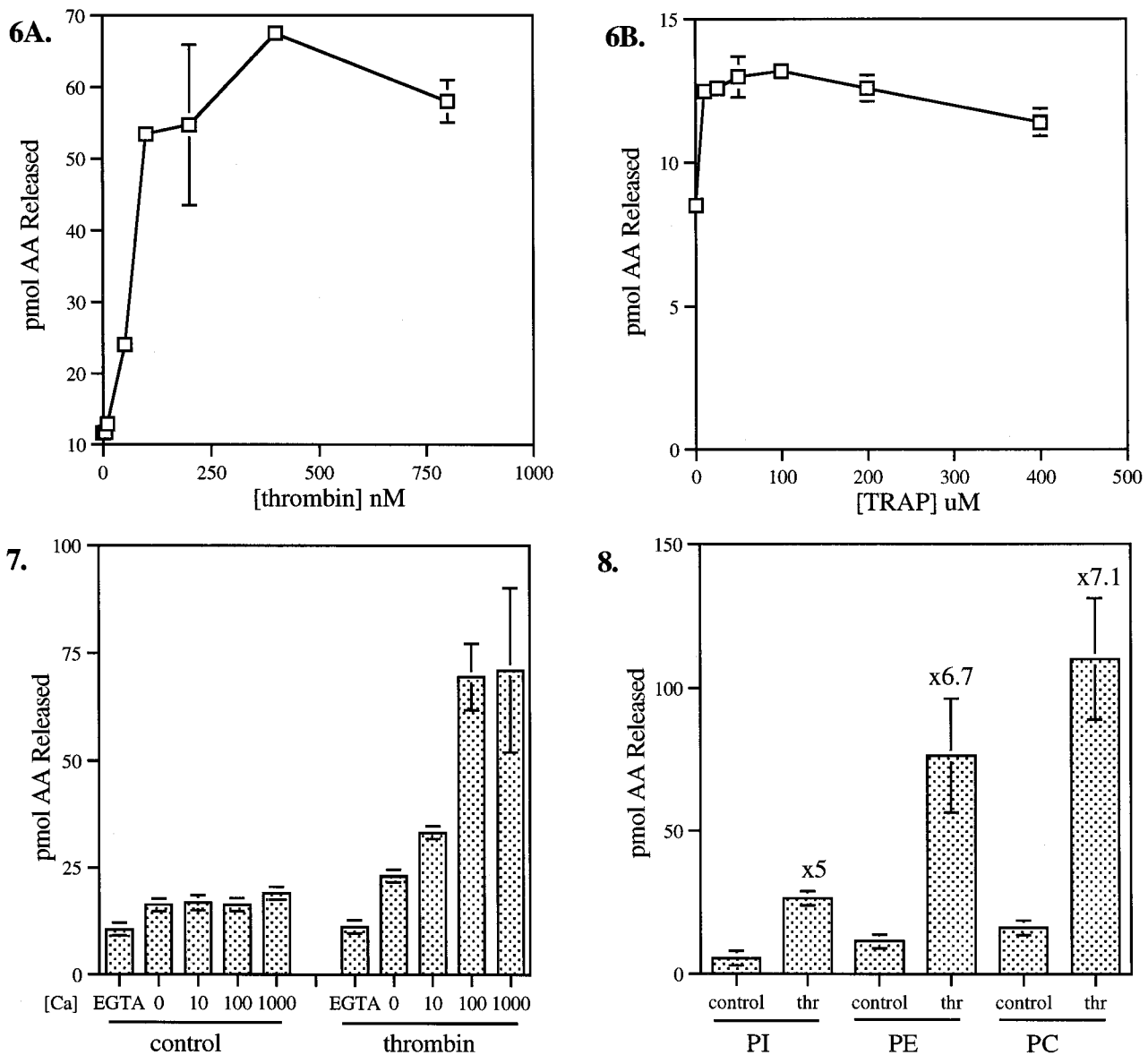
Figure 6. Dose–response curves of PLA$_2$ activation by thrombin (*A*) and TRAP (*B*) in GCPs. GCPs were incubated for 10 min on ice with varying concentrations of thrombin (*A*) or TRAP (*B*) and then for 10 min at 37°C in the reaction mixture in the presence of 10 μM CaCl$_2$. The substrate was [^{14}C]AA-PI. The data presented are net values in triplicate. Error bars represent SD; where not present error bars were too small to be indicated.

Figure 7. Effects of calcium on control and thrombin-stimulated levels of PLA$_2$ in GCPs. GCPs were incubated alone (*control*) or in the presence of 100 nM thrombin for 10 min on ice and then combined with substrate ([^{14}C]AA-PI) for 10 min at 37°C in the presence of EGTA or varying micromolar concentrations of CaCl$_2$ (*0 [Ca]*, no addition of Ca^{2+} or EGTA). AA release was measured as described in Materials and Methods. Data presented are in triplicate. Error bars indicate SD.

Figure 8. Substrate selectivity of thrombin-stimulated growth cone PLA$_2$. GCPs were assayed in the absence (*control*) or presence of 100 nM thrombin (*thr*) with 10 μM CaCl$_2$ and equal concentrations of [^{14}C]AA-PI, -PE, or -PC as substrate. *Numbers* above thrombin columns indicate increase in activity relative to control levels. Absolute values for PE, relative to those for PI, are higher in these experiments compared with those shown in Tables 2–4, because the PE substrate concentration was lower in the latter experiments. However, the degrees of thrombin-induced stimulation were very similar. Data are averages of three experiments, all done in triplicate, $\pm$ SEM.

CDC reduces thrombin-stimulated HETE levels to below control, suggesting that this compound is indeed 12- and/or 15-HETE. This experiment indicates that thrombin stimulates HETE synthesis in GCPs, but it does not discriminate between the activation of PLA$_2$ (shown by increased AA release) and the possible stimulation of LO activity.

To determine whether thrombin regulates LO activity, analogous assays were performed with [^{3}H]AA as the substrate (total AA concentration, ~8 μM). As shown in Figure 11*C*, thrombin does indeed stimulate 12/15-HETE production from AA, and the effect is strongly inhibited by CDC but not by the cyclooxygenase blocker indomethacin. This suggests thrombin activation of 12-LO, in addition to PLA$_2$. However, the amount of 12/15-HETE generated with thrombin stimulation is only a small fraction of the amount of AA released (Fig. 11*A*).

Although TLC is suitable for isolating eicosanoids, identifica-

Table 3. PLA$_2$ activity in neurons and growth cones: effect of reduction on PLA$_2$ activity in GCPs

Condition	Concentration (nM)	Substrate	Net activity (pmol · min^{-1} · mg protein^{-1})	
			No DTT	50 nM DTT
Control		PI	41.9 ± 1.1	66.0 ± 4.7
Thrombin	100	PI	221 ± 39.9	223 ± 53.4

Data are from representative experiment done in triplicate (values are means ± SD). All measurements were obtained in the same experiment and share the control indicated.
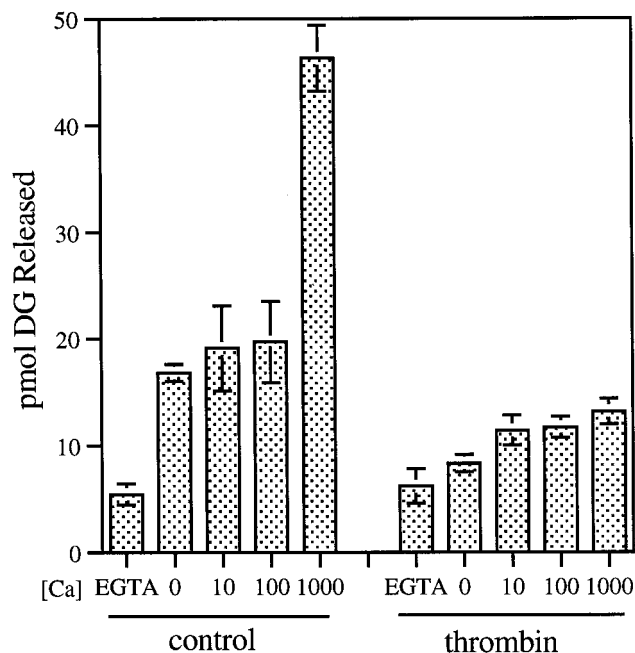

Figure 9. Thrombin inhibits growth cone PLC in a calcium-dependent manner. GCPs were incubated alone (*control*) or in the presence of 100 nM thrombin for 10 min on ice and then combined with substrate ([^{14}C]AA-PI) for 10 min at 37°C in the presence of EGTA or varying micromolar concentrations of CaCl$_2$ (*0 [Ca]*, no addition of Ca^{2+} or EGTA). DG release was measured as described in Materials and Methods. Data presented are triplicates ± SD.

tion of the compounds is tentative only because it is based on co-migration with standards. Therefore, we performed LC–MS–MS to detect specifically the generation of HETE isomers present in GCP extracts after incubation with equal molar quantities of unlabeled and D$_8$-AA. The collisional activation of the common carboxylate anion for the unlabeled isomers (*m/z* 319) and labeled isomers (*m/z* 327) of HETE was performed, and specific ion transitions were monitored to indicate the elution of each HETE species not only by the ion transition but also by the characteristic HPLC retention time. For example, the carboxylate anion from unlabeled 12-HETE was collisionally activated to yield abundant ion at *m/z* 179, whereas the carboxylate anion from labeled 12-HETE was collisionally activated to yield abundant fragmentation at *m/z* 184. The retention times of the elution of these two components (26.1 min) were virtually identical. Using this multiple reaction monitoring technique, 12- and 15-HETE were both found to elute at the appropriate retention times along with the corresponding deuterated species (Fig. 12). The relative
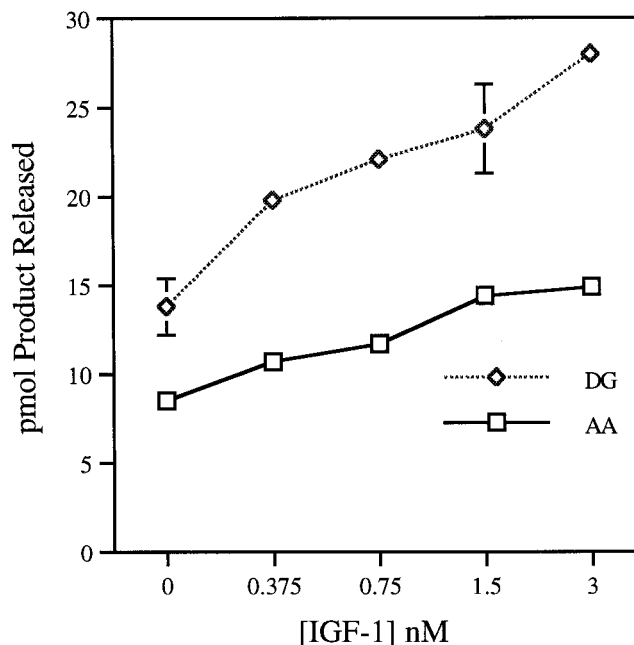

Figure 10. IGF-1 stimulation of PLC and PLA$_2$ in growth cones. GCPs were assayed for both PLA$_2$ and PLC activity as described, in the presence of 10 μM CaCl$_2$ and varying concentrations of IGF-1, using [^{14}C]AA-PI as substrate and recovering [^{14}C]AA and [^{14}C]AA-DG as products. Data are from a representative experiment done in triplicate. Error bars indicate SD; where no error bars appear they were too small to register.

Table 4. PLA$_2$ activity in neurons and growth cones: response of GCPs to different factors

Condition	Concentration (nM)	Substrate	Net activity (pmol · min^{-1} · mg protein^{-1})
Control		PI	107 ± 4
BDNF	100	PI	112 ± 7
IGF-1	0.75	PI	125 ± 10
BDNF + IGF-1	100/0.75	PI	102 ± 8
Insulin	1	PI	106 ± 6

Data are from representative experiment done in triplicate (values are means ± SD). All measurements were obtained in the same experiment and share the control indicated.

quantities of deuterium-labeled species were similar to those of the labeled HETE regioisomers. This supports the conclusion that the origin of recovered HETEs was the exogenous AA added to the GCPs. In separate analyses, known quantities of synthetic 12- and 15-HETE were added to sample aliquots before LC–MS–MS analysis. The corresponding transitions at the appropriate retention time increased for each of the expected HETE regioisomers (data not shown). These techniques revealed the generation in GCPs of both 12- and 15-HETE but could not assign the chirality of each regioisomer.

The generation of 12- and 15-HETE by growth cones, the inhibition of this synthesis by CDC (at 0.156 μM), and the inhibition of the thrombin effect on growth cone morphology by CDC suggest that growth cones contain one or several forms of 12-LO. To test for this possibility, we analyzed GCPs by Western blot with the two 12-LO antibodies currently available, specific for platelet 12-LO and leukocyte 12/15-LO, respectively. Gels con-
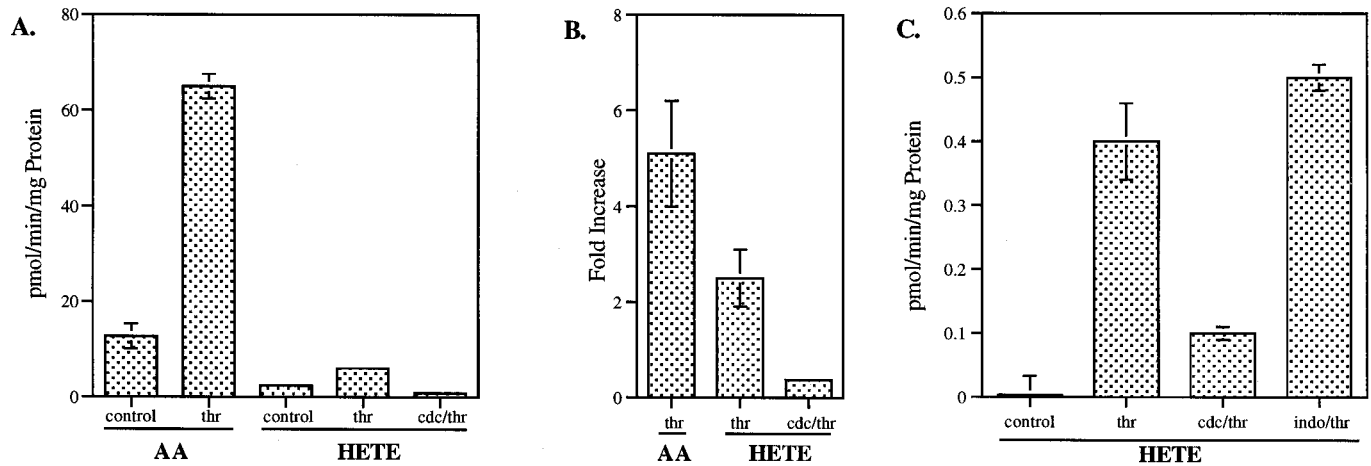
Figure 11. Thrombin-stimulated release of AA and HETE. GCPs were assayed for both PLA_2 and LO activity as described. Inhibitor (0.156 μM CDC or 0.2 μM indomethacin) was introduced to some GCP samples for 15 min on ice before the addition of 100 nM thrombin. After an additional 10 min incubation on ice, the GCP mixture was then incubated with either [^{14}C]AA-PC (*A, B*) or [^{3}H]AA (*C*) in the presence of 10 μM $CaCl_2$ for 15 min at 37°C. *A, B,* Thrombin-stimulated release of AA and HETE in assays using the PC substrate, shown as actual amounts (*A*) and fold increase (*B*). *C,* Thrombin stimulation of HETE directly from the AA substrate. In *A* and *B*, values for control and thrombin-stimulated conditions were averaged from six experiments, all done in triplicate, whereas the values for CDC and indomethacin-treated GCPs were averaged from two experiments, done in triplicate. Data in *C* are from one representative experiment, done in triplicate. Error bars indicate SD; where not seen, they were too small to be shown.
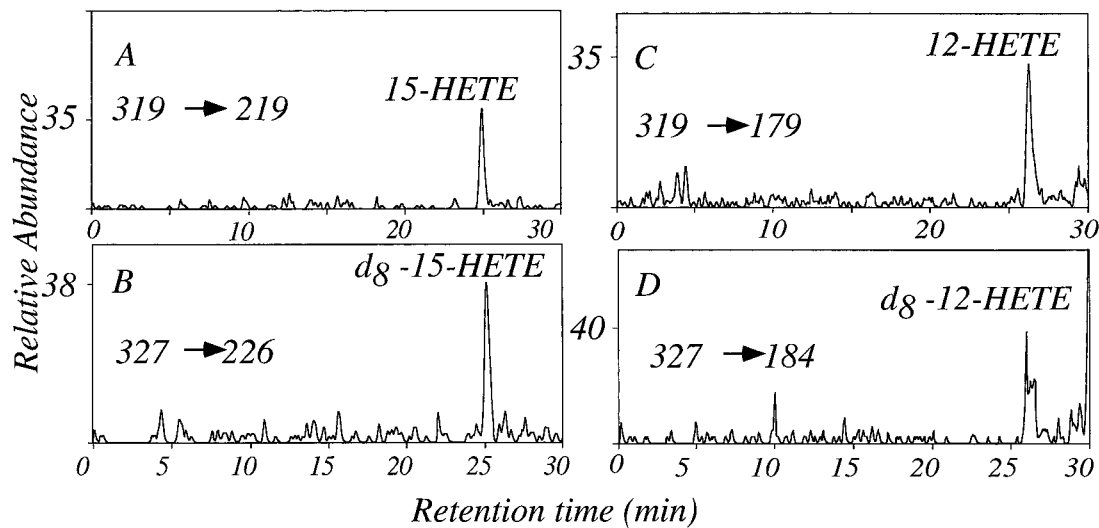

Figure 12. Growth cones synthesize 12- and 15-HETE, as demonstrated by LC–MS–MS. Lipid extracts from growth cones incubated with equal molar quantities of unlabeled and deuterium-labeled (*d_8*) arachidonic acid were resolved by reverse-phase HPLC, and the eluted fractions were analyzed by tandem MS. *A,* LC–MS–MS corresponding to the collisional activation of m/z 319, yielding the ion at m/z 219, which corresponds to 15-HETE. *B,* Collisional activation of m/z 327, yielding product ions at m/z 226, which correspond to D_8-15-HETE. *C,* Collisional activation of m/z 319, yielding product ions at m/z 179, which correspond to 12-HETE. *D,* Collisional activation of m/z 327, yielding product ions at m/z 184, which correspond to D_8-12-HETE.

tained equal amounts of protein from fetal-brain low-speed supernatant (LSS, the crude parent fraction of GCPs) and GCPs. The blots in Figure 13 indicate that GCPs are significantly enriched, relative to LSS, in a protein of ~75 kDa and reactive with the antibody to leukocyte 12/15-LO. No immunoreactivity was detected with anti-platelet 12-LO antibody (data not shown).

DISCUSSION

Thrombin as a growth cone repellent

Thrombin receptor activation leads to diverse cellular responses, such as secretion and pseudopod spreading in platelets and loco-

motion and mitogenesis in fibroblasts. However, it causes cell rounding in endothelial and neural cells and pseudopod withdrawal in certain cancer cells (Jalink and Moolenaar, 1992; Grand et al., 1996; Vouret-Craviari et al., 1998) (S. Ross, B. Essary, B. A. de la Houssaye, X. Pan, K. Mikule, O. Mubarak, and K. H. Pfenninger, unpublished results). In neurons, thrombin induces growth cone collapse comprising redistribution and partial depolymerization of the actin skeleton as well as detachment of filopodia and lamellipodia. This is very similar to collapse induced by other factors (Kapfhammer and Raper, 1987; Fan et al., 1993). TRAP mimics the effect of thrombin, indicating that this is
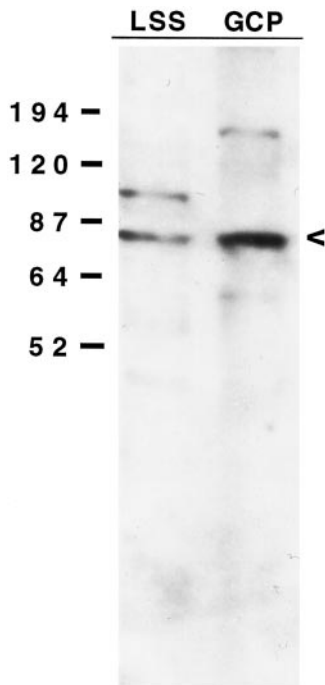
Figure 13. Western blot of GCP polypeptides probed with an antibody to leukocyte 12/15-LO. Equal amounts of protein (30 μg/lane) of LSS and pelleted GCPs were analyzed. The *arrowhead* indicates a 75 kDa band corresponding to the molecular weight of 12/15-LO. Note that the 75 kDa band is enriched in the GCP lane.

a receptor-mediated event, not dependent on proteolysis of adhesion molecules or their extracellular ligands (Jalink and Moolenaar, 1992; Suidan et al., 1992). Thus, thrombin qualifies as a bona-fide collapsing factor and repellent.

Activation of phospholipase and lipoxygenase

In platelets, thrombin activates both cPLA$_2$ and PLC (for review, see Grand et al., 1996). It seemed logical, therefore, to assay for these enzymes in cultures of thrombin-responsive primary neurons. Isolated growth cones were of particular interest in view of the enrichment of at least two different cPLA$_2$s in them (Nègre-Aminou et al., 1996; whether the two enzymes occur separately in distinct growth cone populations or together in all GCPs is unknown).

Thrombin and, to a lesser extent, TRAP stimulate PLA$_2$ activity in primary neurons and GCPs, with the highest levels of free AA achieved in GCPs. Growth factors whose receptors are present on GCPs, such as BDNF, NGF, insulin, and IGF-1, stimulate growth cone cPLA$_2$ only weakly or not at all, indicating that thrombin activation is selective. Thrombin increases AA release from phospholipid from sevenfold to fivefold, with the apparent substrate preference PC > PE > PI. Again, this result does not take into account differences in endogenous substrate concentration and/or possible competition among the PLA$_2$s for the substrate. Resting as well as stimulated levels of PLA$_2$ activity are resistant to reducing agents, excluding a contribution of secreted PLA$_2$. PC hydrolysis had not previously been detected in unstimulated GCPs (Nègre-Aminou et al., 1996). Thus, present results suggest that a third, PC-selective cPLA$_2$ may possibly exist in GCPs. We show that thrombin activation of cPLA$_2$ requires Ca^{2+}. However, Nègre-Aminou et al. (1996) reported PE- and PI-selective cPLA$_2$s to be Ca^{2+}-independent. Therefore, Ca^{2+} is likely to be necessary for a step upstream of cPLA$_2$.

Although growth cones and platelets share receptor-mediated thrombin stimulation of cPLA$_2$, they are different with regard to PLC regulation. Thrombin stimulates platelet PLC, causing the release of inositol trisphosphate and subsequent efflux of Ca^{2+} from intracellular stores. In GCPs, however, thrombin inhibits this phosphoinositidase, suggesting that intracellular release of Ca^{2+} is not important for the collapse response. Thrombin-induced Ca^{2+} transients have been reported for platelets (Grand et al., 1996) and neuroblastoma cells (Jalink and Moolenaar, 1992), but they were shown *not* to be necessary for thrombin-induced rounding of neuroblastoma and endothelial cells (Jalink and Moolenaar, 1992; Vouret-Craviari et al., 1998). Therefore, our findings are consistent with these observations as well as the fact that (at least so far) Ca^{2+} transients have not been detectable in nerve growth cones treated with repellents (Ivins et al., 1991; Ming et al., 1997). The second consequence of PLC stimulation, the release of DG, activates PKC in platelets. Lack of PLC stimulation in thrombin-treated GCPs, however, does not rule out a role for PKC in repellent action.

cPLA$_2$s cleave phospholipids into an unsaturated fatty acid, in brain typically AA, and a lysophospholipid. Whether lyso-PI, -PE, and -PC generated in growth cones have functional role(s) is not known. Most released AA is rapidly reincorporated into phospholipid (Nègre-Aminou and Pfenninger, 1993), but AA may directly influence growth cone functions and/or may be converted into one or more eicosanoids (Smith, 1989; Shimizu and Wolfe, 1990). Our biochemical studies show that thrombin stimulates in growth cones not only the release of AA but also the synthesis of an AA-derived compound that co-extracts and co-migrates in TLC with 12- or 15-HETE. The generation of this product is reduced by the selective 12-LO inhibitor CDC but not by the cyclooxygenase inhibitor indomethacin. Finally, LC–MS–MS analysis of GCP extracts definitively demonstrates GCP synthesis of primarily 12- and also 15-HETE.

In sum, our results demonstrate strong and selective thrombin stimulation of one or multiple cPLA$_2$s in growth cones, followed by conversion of some of the released AA into 12/15-HETE. We estimate the conversion to amount to ~1 pmol, or 5%, of ~20 pmol of AA released in the same assay (assuming equal recoveries). Although we cannot exclude a role of 15-LO in GCPs, HETEs are likely to be synthesized by 12-LO because of the selective inhibitory effect of CDC at 0.156 μm (Cho et al., 1991) and a report that leukocyte 12/15-LO also generates 15-HETE (Yamamoto et al., 1997). This view is consistent with the observation that growth cones are enriched in a polypeptide that co-migrates in SDS-PAGE with 12-LO (at 75 kDa) and immuno-cross-reacts with an antibody to leukocyte-type 12/15-LO (but not platelet 12-LO).

It is generally assumed that eicosanoid synthesis, including that of 12-HETE, is regulated by the supply of AA, and that 12-LO is constitutively active (Smith, 1989; Shimizu and Wolfe, 1990; Yamamoto et al., 1997). However, we observed that thrombin stimulates not only cPLA$_2$ but also the 12-LO in GCPs.

Functional role of lipid messengers in growth cone collapse

The data discussed so far correlate the collapsing effect of thrombin with cPLA$_2$ activation and eicosanoid synthesis. To determine whether a causal relationship exists, inhibitor experiments were performed. Selective inhibitors of most or all growth cone cPLA$_2$ activity are not known, but specific eicosanoid synthesis inhibitors exist. The cyclooxygenase inhibitor indomethacin does

not interfere with thrombin-induced growth cone collapse. However, the general LO inhibitor NDGA and the specific 12-LO inhibitor CDC block thrombin- and TRAP-induced collapse, as well as LO activity in biochemical assays. Conversely, exogenous 12(S)-HETE added to cultures mimics the effects of thrombin or TRAP. These results are consistent with the observed thrombin stimulation of 12/15-HETE synthesis and link cPLA$_2$ activation and 12/15-HETE synthesis functionally to the collapse mechanism.

Growth cone collapse involves reorganization of the actin cytoskeleton as well as filopodial and lamellipodial detachment. Our detachment assay demonstrates that thrombin and TRAP trigger growth cone dissociation from the laminin substratum, even in the absence of a functional actin cytoskeleton. Disassembly of the actin cytoskeleton with cytochalasin D or inhibition of myosin ATPase with BDM interferes to some degree with GCP adhesion. However, release induced by thrombin plus blocker of the actin cytoskeleton approximates the sum of thrombin alone plus the actin function blocker alone. Thus, BDM and cytochalasin D do not block thrombin-induced detachment. This observation is complemented by the finding that growth cones pretreated with CDC and then challenged with thrombin sometimes contain peripherally depleted and proximally condensed F-actin, even though they retain their spread-out, attached filopodia and overall shape. Together these findings may suggest that cPLA$_2$ and leukocyte 12/15-LO are involved primarily in triggering detachment rather than cytoskeletal redistribution.

In conclusion, our data indicate that thrombin is a growth cone repellent that triggers not only redistribution of the actin cytoskeleton but also detachment of filopodia and lamellipodia. Our results indicate further that thrombin-induced growth cone collapse occurs by a mechanism that involves cPLA$_2$ and 12/15-LO. The mode of action of 12/15-HETE is not known, but our preliminary data suggest the involvement of PKC activation and phosphorylation of the adhesion site-associated protein, MARCKS (myristoylated alanine-rich C-kinase substrate), which may trigger disassembly of attachment sites (de la Houssaye et al., 1997; Mikule et al., 1997).

REFERENCES

Bar-Sagi D (1989) Phospholipase A$_2$ in ras-transformed cells. In: Cell activation and signal initiation: receptor and phospholipase control of inositol phosphate, PAF, and eicosanoid production (Dennis EA, Hunter T, Berridge M, eds), pp 331–335. New York: Liss.

Bar-Sagi D, Feramisco JR (1986) Induction of membrane ruffling and fluid-phase pinocytosis in quiescent fibroblasts by ras proteins. Science 233:1061–1068.

Birkle DL, Bazan EP, Bazan NG (1988) Analysis of prostaglandins, leukotrienes, and related compounds in retina and brain. In: Neuromethods, Vol 7 (Boulton AA, Baker GB, Horrocks LA, eds), pp 227–244. Totowa: NJ: Humana.

Bligh EG, Dyer WJ (1959) A rapid method of total lipid extraction and purification. Can J Biochem Physiol 37:911–917.

Bradford MM (1976) A rapid and sensitive method for the quantification of microgram quantities of protein utilizing the principle of protein-dye binding. Anal Biochem 72:248–254.

Brennan C, Monschau B, Lindberg R, Guthrie B, Drescher U, Bonhoeffer, Holder N (1997) Two Eph receptor tyrosine kinase ligands control axon growth and may be involved in the creation of the retinotectal map in the zebrafish. Development 124:655–664.

Capdevila JH, Falck JR, Estabrook RW (1992) Cytochrome P450 and the arachidonate cascade. FASEB J 6:731–736.

Cho H, Ueda M, Tamaoka M, Hamaguchi M, Aisaka K, Kiso Y, Inoue T, Ogino R, Tatsuoka T, Ishihara T, Noguchi T, Morita I, Murota S (1991) Novel caffeic acid derivatives: extremely potent inhibitors of 12-lipoxygenase. J Med Chem 34:1503–1505.

Cramer LP, Mitchison TJ (1995) Myosin is involved in postmitotic cell spreading. J Cell Biol 131:179–189.

Crouch MF, Lapetina EG (1988) A role for G$_i$ in control of thrombin receptor-phospholipase C coupling in human platelets. J Biol Chem 263:3363–3371.

de la Houssaye BA, Mikule K, Ross S, Pfenninger KH (1997) Thrombin-triggered pseudopod detachment in nerve growth cones and motile cancer cells. Mol Biol Cell 8:265a.

Dennis EA (1994) Diversity of group types, regulation, and function of phospholipase A$_2$. J Biol Chem 269:13057–13060.

Drescher U, Kremoser C, Handwerker C, Loschinger J, Noda M, Bonhoeffer F (1995) In vitro guidance of retinal ganglion cell axons by RAGS, a 25 kDa tectal protein related to ligands for Eph receptor tyrosine kinases. Cell 82:359–370.

Fan J, Mansfield G, Redmond T, Gordon-Weeks PR, Raper JA (1993) The organization of F-actin and microtubules in growth cones exposed to a brain-derived collapsing factor. J Cell Biol 121:867–878.

Feng D-M, Veber DF, Connolly TM, Condra C, Tang M-J, Nutt RF (1995) Development of a potent thrombin receptor ligand. J Med Chem 38:4125–4130.

Ferrante A, Goh D, Harvey D, Robinson B, Hii CS, Bates E, Hardy SJ, Johnson DW, Poulos A (1994) Neurtophil migration inhibitory properties of polyunsaturated fatty acids. J Clin Invest 93:1063–1070.

Gallo G, Letourneau PC (1998) Axon guidance: GTPases help axons reach their targets. Curr Biol 8:R80–R82.

Gebbink M, Kranenburg O, Poland M, van Horck FPG, Houssa B, Moolenaar WH (1997) Identification of a novel, putative Rho-specific GDP/GTP exchange factor and a RhoA-binding protein: control of neuronal morphology. J Cell Biol 137:1603–1613.

Goetzl EJ, Woods JM, Gorman RR (1977) Stimulation of human eosinophil and neutrophil polymorphonuclear leukocyte chemotaxis and random migration by 12-L-hydroxy-5,8,10,14-eicosatetraenoic acid. J Clin Invest 59:179–183.

Grand RJA, Turnell AS, Grabham PW (1996) Cellular consequences of thrombin-receptor activation. Biochem J 313:353–368.

Gurwitz D, Cunningham DD (1988) Thrombin modulates and reverses neuroblastoma neurite outgrowth. Proc Natl Acad Sci USA 85:3440–3444.

Hawkins RL, Seeds NW (1986) Effect of proteases and their inhibitors on neurite outgrowth from neonatal mouse sensory ganglia in culture. Brain Res 398:63–70.

Hawkins RL, Seeds NW (1989) Protease inhibitors influence the direction of neurite outgrowth. Dev Brain Res 45:203–209.

Huang R, Sorisky A, Church WR, Simons ER, Rittenhouse SE (1991) "Thrombin" receptor-directed ligand accounts for activation by thrombin of platelet phospholipase C and accumulation of 3-phosphorylated phosphoinositides. J Biol Chem 266:18435–18438.

Huttenlocher A, Sandborg R, Horwitz A (1995) Adhesion in cell migration. Curr Opin Cell Biol 7:697–706.

Igarashi M, Strittmatter SM, Vartanian T, Fishman MC (1993) Mediation by G proteins of signals that cause collapse of growth cones. Science 259:77–79.

Ishihara H, Connolly AJ, Zeng D, Kahn ML, Zheng YW, Timmons C, Tram T, Coughlin SR (1997) Protease-activated receptor 3 is a second thrombin receptor in humans. Nature 386:502–506.

Ivins JK, Raper JA, Pittman RN (1991) Intracellular calcium levels do not change during contact-mediated collapse of chick DRG growth cone structure. J Neurosci 11:1597–1608.

Jalink K, Moolenaar WH (1992) Thrombin receptor activation causes rapid neural cell rounding and neurite retraction independent of classic second messengers. J Cell Biol 118:411–419.

Jalink K, van Corven EJ, Hengeveld T, Morii N, Narumiya S, Moolenaar WH (1994) Inhibition of lysophosphatidate- and thrombin-induced neurite retraction and neuronal cell rounding by ADP ribosylation of the small GTP-binding protein Rho. J Cell Biol 126:801–810.

Jin Z, Strittmatter SM (1997) Rac1 mediates collapsin-1-induced growth cone collapses. J Neurosci 17:6256–6263.

Kapfhammer JP, Raper JA (1987) Interactions between growth cones and neurites growing from different neural tissues in culture. J Neurosci 7:1595–1600.

Katoh H, Aoki J, Ichikawa A, Negishi M (1998) p160 RhoA-binding kinase ROKa Induces Neurite Retraction. J Biol Chem 273:2489–2492.

Laemmli UK (1970) Cleavage of structural proteins during assembly of the head of the bacteriophage T4. Nature 227:680–685.

Lamoureux P, Altun-Gultekin ZF, Lin C, Wagner JA, Heidemann SR

(1997) Rac is required for growth cone function but not neurite assembly. J Cell Sci 110:635–641.

Lockerbie RO, Miller VE, Pfenninger (1991) Regulated plasmalemmal expansion in nerve growth cones. J Cell Biol 112:1215–1227.

Lohse K, Helmke SM, Wood MR, Quiroga S, de la Houssaye B, Miller VE, Nègre-Aminou P, Pfenninger, KH (1996) Axonal origin and purity of growth cones isolated from fetal rat brain. Dev Brain Res 96:83–96.

Lowry OH, Rosebrough NJ, Farr AL, Randall RJ (1951) Protein measurement with the Folin phenol reagent. J Biol Chem 193:265–275.

MacMillan DK, Murphy RC (1995) Analysis of lipid hydroperoxides and long-chain conjugated keto acids by negative ion electrospray mass spectrometry. J Am Soc Mass Spectrom 6:1190–1201.

Mansuy IM, van der Putten H, Schmid P, Meins M, Botteri FM, Monard D (1993) Variable and multiple expression of protease nexin-1 during mouse organogenesis and nervous system development. Development 119:1119–1134.

Mikule K, de la Houssaye BA, Pfenninger KH (1997) Collapsin signalling involves phospholipase A_2 activation. Soc Neurosci Abstr 23:600.

Ming GL, Song HJ, Berninger B, Holt C, Tessier-Lavigne M, Poo M-m (1997) cAMP-dependent growth cone guidance by netrin-1. Neuron 19:1225–1235.

Monard D (1988) Cell-derived proteases and protease inhibitors as regulators of neurite outgrowth. Trends Neurosci 11:541–544.

Monard, D, Niday E, Limat A, Solomon F (1983) Inhibition of protease activity can lead to neurite extension in neuroblastoma cells. Prog Brain Res 58:359–364.

Moolenaar WH, Kranenburg O, Postma FR, Zondag GCM (1997) Lysophosphatidic acid: G-protein signalling and cellular responses. Curr Opin Cell Biol 9:168–173.

Mooney DJ, Langer R, Ingber DE (1995) Cytoskeletal filament assembly and the control of cell spreading and function by extracellular matrix. J Cell Sci 108:2311–2320.

Nataranjan S, Riexinger D, Peluso M, Sieler SM (1995) Tethered ligand derived pentapeptide agonists of thrombin receptor: a study of side chain requirements for human platelet activation and GTPase stimulation. Int J Peptide Res 45:145–151.

Nègre-Aminou P, Pfenninger KH (1993) Arachidonic acid turnover and phospholipase A_2 activity in neuronal growth cones. J Neurochem 60:1126–1136.

Nègre-Aminou P, Nemenoff RA, Wood MR, de la Houssaye BA, Pfenninger KH (1996) Characterization of phospholipase A_2 activity enriched in the nerve growth cone. J Neurochem 67:2599–2608.

Niclou S, Suidan HS, Brown-Luedi M, Monard D (1994) Expression of the thrombin receptor mRNA in rat brain. Cell Mol Biol 40:421–428.

Peterson GL (1983) Determination of total protein. Methods Enzymol 91:95–119.

Pfenninger KH, Maylié-Pfenninger M-F (1981) Lectin labelling of sprouting neurons. I. Regional distribution of surface glycoconjugates. J Cell Biol 89:536–546.

Pfenninger KH, Ellis L, Johnson MP, Friedman LB, Somlo S (1983) Nerve growth cones isolated from fetal rat brain: subcellular fractionation and characterization. Cell 35:573–584.

Poiraudeau S, Lieberherr M, Kergosie N, Corvol MT (1997) Different mechanisms are involved in intracellular calcium increase by insulin-like growth factors 1 and 2 in articular chondrocytes: voltage-gated calcium channels, and/or phospholipase C coupled to a pertussis-sensitive G-protein. J Cell Biochem 64:414–422.

Quiroga S, Garofalo R, Pfenninger KH (1995) Insulin-like growth factor I receptors of fetal brain are enriched in nerve growth cones and contain a β-subunit variant. Proc Natl Acad Sci USA 92:4309–4312.

Salari H, Braquet P, Borgeat P (1984) Comparative effects of indomethacin, acetylenic acids, 15-HETE, nordihydroguaiaretic acid and BW755C on the metabolism of arachidonic acid in human leukocytes and platelets. Prostaglandins Leukot Med 13:53–60.

Sanders LC, Matsumura F, Bokoch GM, de Lanerolle P (1999) Inhibition of myosin light chain kinase by p21-activated kinase. Science 283:2083–2085.

Schindelholz B, Reber BFX (1997) Bradykinin-induced collapse of rat pheochromocytoma (PC12) cell growth cones: a role for tyrosine kinase activity. J Neurosci 17:8391–8401.

Schwab ME (1990) Myelin-associated inhibitors of neurite growth and regeneration in the CNS. Trends Neurosci 13:452–456.

Shimizu T, Wolfe LS (1990) Arachidonic acid cascade and signal transduction. J Neurochem 55:1–15.

Smalheiser NR, Ali JY (1994) Acute neurite retraction triggered by lysophosphatidic acid: timing of the inhibitory effects of genistein. Brain Res 600:309–318.

Smith W (1989) Eicosanoids and their biochemical mechanisms of action. Biochem J 259:315–324.

Stossel TP (1993) On the crawling of animal cells. Science 260:1086–1094.

Suidan HS, Stone SR, Hemmings BA, Monard D (1992) Thrombin causes neurite retraction in neuronal cells through activation of cell surface receptors. Neuron 8:363–375.

Tang DG, Timar J, Grossi IM, Renaud C, Kimler VA, Diglio CA, Taylor JD, Honn KV (1993) The lipoxygenase metabolite, 12(*S*)-HETE, induces a protein kinase C-dependent cytoskeletal rearrangement and retraction of microvascular endothelial cells. Exp Cell Res 207:361–375.

Tapon N, Hall A (1997) Rho, Rac and Cdc42 GTPases regulate the organization of the actin cytoskeleton. Curr Opin Cell Biol 9:86–92.

Teslenko V, Rogers M, Lefkowith JB (1997) Macrophage arachidonate release via both the cytosolic Ca^{2+}-dependent and -independent phospholipases is necessary for cell spreading. Biochim Biophys Acta 1344:189–199.

Tessier-Lavigne M, Goodman CS (1996) The molecular biology of axon guidance. Science 274:1123–1133.

Towbin H, Staehelin T, Gordon J (1979) Electrophoretic transfer of proteins from polyacrylamide gels to nitrocellulose sheets: procedure and some applications. Proc Natl Acad Sci USA 76:4350–4354.

Vouret-Craviari V, Boquet P, Pouysségur J, Van Obberghen-Schilling E (1998) Regulation of the actin cytoskeleton by thrombin in human endothelial cells: role of Rho proteins in endothelial barrier function. Mol Biol Cell 9:2639–2653.

Vu TK, Hung DT, Wheaton VI, Coughlin SR (1991) Molecular cloning of a functional thrombin receptor reveals a novel proteolytic mechanism of receptor activation. Cell 64:1057–1068.

Weinstein JR, Gold SJ, Cunningham DD, Gall CM (1995) Cellular localization of thrombin receptor mRNA in rat brain: expression by mesencephalic dopaminergic neurons and codistribution with prothrombin mRNA. J Neurosci 15:2906–2919.

Wen Y, Nadler JL, Gonzales N, Scott S, Clauser E, Natarangan R (1996) Mechanisms of ANG II-induced mitogenic responses: role of 12-lipoxygenase and biphasic MAP kinase. Am J Physiol 271: C1212–C1220.

Yamamoto S, Suzuki H, Ueda N (1997) Arachidonate 12-lipoxygenases. Prog Lipid Res 36:23–41.

Yoshino H, Kitayama S, Morita K, Okamoto H, Tsujimoto A, Dohi T (1993) 12-Lipoxygenase product as an inhibitor of the action of chemoattractant peptide fMet-Leu-Phe in rat neutrophils. Gen Pharmacol 24:1249–1251.

Zipkin LD, Kindt RM, Kenyon CJ (1997) Role of a new Rho family member in cell migration an axon guidance in *C. elegans*. Cell 90:883–894.